Crystallization in Emulsions: A Thermo-Optical Method to Determine Single Crystallization Events in Droplet Clusters

Serghei Abramov *, Patrick Ruppik and Heike Petra Schuchmann

Karlsruhe Institute of Technology (KIT), Institute of Process Engineering in Life Sciences,
Section I: Food Process Engineering (LVT), Kaiserstr. 12, 76131 Karlsruhe, Germany;
heike.schuchmann@kit.edu (H.P.S.)
* Correspondence: serghei.abramov@kit.edu; Tel.: +49-721-608-42497

Abstract: Delivery systems with a solid dispersed phase can be produced in a melt emulsification process. For this, dispersed particles are melted, disrupted, and crystallized in a liquid continuous phase (melt emulsification). Different to bulk crystallization, droplets in oil-in-water emulsions show individual crystallization behavior, which differs from droplet to droplet. Therefore, emulsion droplets may form liquid, amorphous, and crystalline structures during the crystallization process. The resulting particle size, shape, and physical state influence the application properties of these colloidal systems and have to be known in formulation research. To characterize crystallization behavior of single droplets in micro emulsions (range 1 μm to several hundred μm), a direct thermo-optical method was developed. It allows simultaneous determination of size, size distribution, and morphology of single droplets within droplet clusters. As it is also possible to differentiate between liquid, amorphous, and crystalline structures, we introduce a crystallization index, CI_i, in dispersions with a crystalline dispersed phase. Application of the thermo-optical approach on hexadecane-in-water model emulsion showed the ability of the method to detect single crystallization events of droplets within emulsion clusters, providing detailed information about crystallization processes in dispersions.

Keywords: melt emulsification; emulsion crystallization; thermo-optical colloid analysis; crystallization index

1. Introduction

The development of novel delivery systems for bioactive substances has a wide field of applications in food [1], cosmetic [2], and pharmaceutical [3] industries. Many of those organic active substances are either unstable, and/or insoluble in water and consequently have low bioavailability. Especially targeting and influencing release kinetics is a great challenge. Encapsulation of these substances in colloidal lipophilic systems, such as emulsions, allows an application in aqueous solutions for use in human bodies or other life science systems [4,5]. The transformation of such emulsions into suspensions enables a further specialization. The solid state of the obtained colloids allows surface functionalization and diffusion controlled release for site-specific and adjusted release kinetics of bioactive substances [6–8].

Colloidal delivery systems with a crystalline dispersed phase can be produced in a two-step melt emulsification process [9]. In the first step, the dispersed phase is emulsified above its melting temperature in a mechanical or thermo-physical emulsification process. In the second step, the droplets are cooled down until crystallization occurs and the emulsion forms a fine dispersed suspension [10–12]. While bulk crystallization is quite well understood today, crystallization

of molten droplets in emulsions poses challenges [13]. Different to bulk crystallization, organic droplets in oil-in-water emulsions show individual crystallization behavior which differs from droplet to droplet. During supercooling, droplets can remain as supercooled liquid, form amorphous particles, or crystallize as mono and multi crystalline structures. The ormation of different structures within emulsions during crystallization depends on the materials used, the thermal energy, and external forces which influence nucleation in emulsions [14]. For example, surfactants may initiate heterogeneous nucleation at the interface and influence the form of particles after crystallization [15,16], collisions cause secondary heterogeneous nucleation and increase nucleation rates [17,18], and shear stress can influence nucleation mechanisms by forming shear-dependent crystalline structures [19,20]. Therefore, resulting particle size, shape, and physical state of dispersions after cooling depend on the formulation and on the melt emulsification process itself, and can eventually influence application properties such as bioavailability, drug loading, and release behavior of colloidal delivery systems [21,22].

Apart from life science systems, solidification of droplets occurs in a number of industrial applications, such as formulations of mold release agents, mini emulsion polymerization (including semi crystalline polymers), or hydrate formation in droplets during pipeline transport of crude oil [23,24]. Therefore, various methods to characterize crystallization behavior, crystal structure, and solid fraction in emulsions were developed and established in the past decades [25–31]. Commonly used methods are based on differential scanning calorimetry [32], ultrasound velocimetry [33], and X-ray diffraction [34]. Unfortunately, those methods describe integral quantities and are not able to detect crystallization events in single droplets or to differentiate between crystallization events in different single droplets within emulsions.

In this contribution, we propose a novel direct thermo-optical method that was developed to: (1) describe the crystallization behavior of droplets in the range of 1 μm to several hundred μm in concentrated micro emulsions, and (2) to detect and characterize individual crystallization events in single droplets of droplet clusters. At the same time, the determination of particle size, size distribution, and morphology—with additional differentiation between liquid, amorphous, and crystalline structures—enables the introduction of the crystallization index, CI_i. We applied the thermo-optical analysis to a hexadecane oil-in-water model emulsion stabilized with Tween® 20, and compared the results with calorimetric measurements of crystallization behavior within the dispersion. Using our thermo-optical approach, we were able to detect single crystallization events within droplet clusters and differentiate in our model emulsion between liquid, supercooled liquid, and multi-crystalline states of the dispersion during the crystallization process.

2. Experimental Section

2.1. Materials

All substances used were commercially available and used as obtained without further purification or processing, unless otherwise noted. Hexadecane (purity 99%, melting point at 18 °C) was purchased from Sigma-Aldrich® (St. Louis, MO, USA) and polyoxyethylen-20-sorbitanmonolaurat (Tween® 20) was purchased from Carl-Roth® (Karlsruhe, Germany). Water was purified in a Milli-Q® instrument (Q-POD®, 18.2 MΩ) (Darmstadt, Germany).

2.2. Emulsion Preparation

Every emulsion was prepared three times for triple determination and consisted of 1 wt % hexadecane (dispersed phase), 1 wt % Tween® 20 (surfactant), and 98 wt % Milli-Q water (continuous phase). First, Tween® 20 was dissolved in tempered Milli-Q water at 28 °C (10 K above melting point of hexadecane) and stirred for 10 min at 28 °C in a glass vessel of 25 mm inner diameter. Afterwards, hexadecane was added to the surfactant solution and tempered with a tooth-rim dispersing element for an additional 15 min at 28 °C without stirring. Then, hexadecane was dispersed

with a tooth-rim dispersing machine (IKA® T25 digital, ULTRA-TURRAX®, Staufen im Breisgau, Germany) at 2.2 m/s tangential speed (3200 rpm, 13 mm rotor outer diameter) 10 K above its melting point for 10 min. After emulsification, samples were taken for differential scanning calorimetry (DSC), laser diffraction/droplet size measurements, and thermo-optical polarized microscopy analysis. Between emulsification and analysis, the emulsions were continuously stirred to avoid creaming/inhomogeneous sampling and kept above the melting temperature of hexadecane (18 °C). During the experimental part, emulsions did not show any sign of instability.

2.3. Characterization of Emulsions and Crystallization Behavior

2.3.1. Differential Scanning Calorimetry Analysis

For thermal analysis, samples of bulk hexadecane (between 5 and 6 mg) and samples of hexadecane-in-water emulsions (between 9 and 10 mg) were weighed and sealed in aluminum pans. Samples with bulk hexadecane and hexadecane emulsions were then loaded in a differential scanning calorimeter (DSC 8000, Perkin Elmer, Waltham, MA, USA) and cooled from 25 to 0 °C with a cooling rate of 1 K/min. Afterwards, samples were heated from 0 to 25 °C with a heating rate of 1 K/min. The DSC apparatus had previously been calibrated against n-decane and indium. Every sample was run against an empty aluminum pan. Differential scanning calorimetry measurements were performed to measure the solid fraction and the onset phase transition temperature during controlled cooling and heating of bulk hexadecane and 1 wt % hexadecane in Milli-Q water emulsions stabilized with 1 wt % Tween® 20. Therefore, the heat flows of bulk hexadecane and hexadecane oil-in-water emulsions were recorded as a function of temperature. The peaks of the heat flow curve were used to identify crystallization and melting onset temperature during temperature scans. Peak areas were calculated to quantify the solid fraction during liquid-solid and solid-liquid phase transitions according to McClements [32].

2.3.2. Laser Diffraction Analysis

The droplet size distributions (DSD) of emulsions were determined by a laser diffraction particle size analyzer (HORIBA LA-940, Retsch Technology, Haan, Germany) in a stirred fraction cell. The measuring range of the instrument is between 0.01 and 3000 µm due to data analysis using a combination of laser diffraction and Mie scattering theory. The refractive index used for hexadecane was 1.434 + 0.000i. Emulsions were strongly diluted and measured three times above melting temperature of hexadecane. Measurements of crystallized emulsions were not possible due to the absence of cooling equipment in the stirred fraction cell.

2.3.3. Polarized Microscopy Analysis

The thermo-optical observation of the crystallization behavior of hexadecane-in-water droplets in a droplet collective was investigated using a customized polarizing microscope (Eclipse Ci-L, Nikon, Shinagawa, Tokyo, Japan) equipped with an optically accessible temperature controlled stage (LTS 420, Linkam Scientific, Tadworth, UK).

After the emulsification step, 25 µL of emulsion were pipetted between two microscope cover slips placed on a tempered microscope object slide using a tempered pipette, then covered with a third cover slip and sealed with silicone at 28 °C. Afterwards, the sealed samples were placed in the optically accessible temperature-controlled stage and held at 28 °C until the start of experiment as shown in Figure 1. Time between emulsification and experiment was always less than 15 min.

To investigate the crystallization behavior of droplets in emulsions, sealed samples were cooled down from 28 to 0 °C with cooling rate of 1 K/min. During the entire experiment, picture sequences of the crystallizing dispersion were taken every 0.2 K.
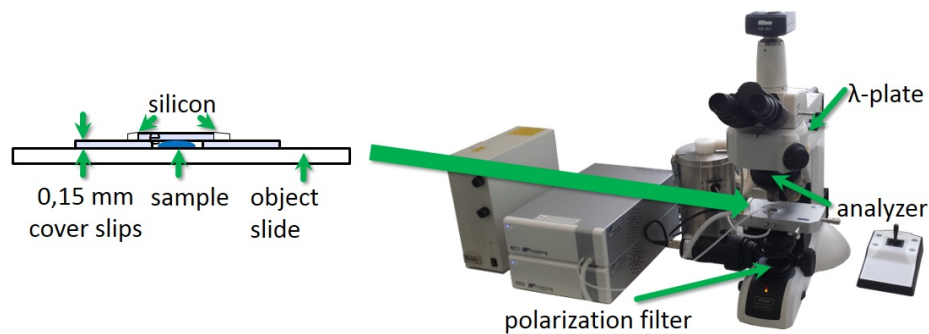
Figure 1. Experimental set up for the thermo-optical investigation of the crystallization behavior of single droplets in droplet clusters. The left image shows the sample preparation procedure. The polarizing light microscope with optically accessible precise cooling and heating stage is shown on the right.

2.3.4. Image Processing

The obtained picture sequences were processed with ImageJ (version 1.46r, National Institute of Health, Bethesda, MD, USA) software to determine characteristic values, such as number, size, and size distribution of crystallized and supercooled droplets as shown in Figure 2.
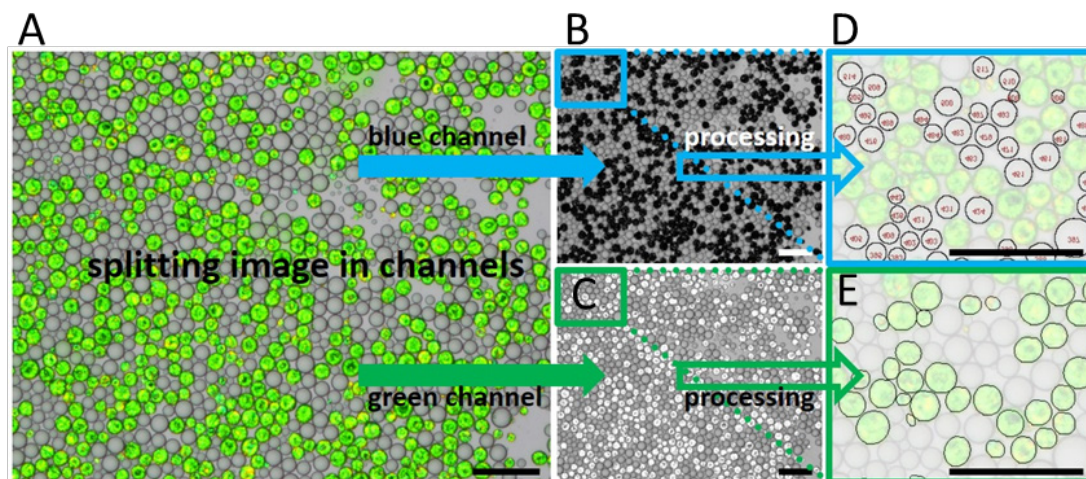

Figure 2. (**A**) shows the original image of 1 wt % hexadecane in Milli-Q water emulsion stabilized with 1 wt % Tween® 20 at 4.7 °C. Gray transparent spheres are liquid, supercooled droplets and green opaque spheroids are multi crystalline structures of solidified hexadecane droplets; (**B**) shows the blue channel of the original image and (**C**) shows the green channel of the original image; (**D**) shows the processed blue channel image with the resulting determination of supercooled droplets by number and area; (**E**) shows the processed green channel image with the resulting determination of crystallized droplets by number and area. Droplets/particles on the edge of the image were excluded from the characterization. Length of the scale bar is 100 μm.

First, the original micrograph was split into red, blue, and green channel images. Due to the green appearance of crystallized droplets, the green channel image (see Figure 2C) of the original image was used to characterize the crystallized droplets by number and area. Therefore, the green channel image was inverted and the threshold was adjusted to exclude supercooled droplets from image processing. Analogous to the characterization of crystallized droplets, the blue channel image (see Figure 2B) was processed to characterize supercooled droplets by number and area, excluding the crystalized particles by inverting the image and adjusting the threshold. To avoid analysis errors, such as not detected or falsely joined droplets and crystals, functions like "fill holes" and "watershed" were applied. Finally,

using shape detecting tools such as "show outlines" or "show ellipses", supercooled droplets (see Figure 2D) and crystallized droplets (see Figure 2E) were characterized by number and area and the surface equivalent diameter of spheres was calculated. Droplets and particles on the edge of the image were excluded from the characterization. Consequently, droplet and particle size distributions were determined according to mechanical engineering and particle technology textbooks, such as [35].

3. Results and Discussion

DSC measurements of bulk hexadecane showed sharp exothermic peaks during cooling (solidification peak) and broader endothermic peaks during heating (melting peak) as shown in Figure 3. The crystallization temperature of bulk hexadecane was determined to be 16.21 °C ($\pm$0.12 K) and the melting temperature to be 18.26 °C ($\pm$0.05 K) as shown in Table 1. Due to the exothermic nature of crystallization, the solid content increased nearly instantaneously from zero (no solidification) to one (fully solidification) within 1 K at crystallization temperature, and is shown in Figure 3 as a dot chain line.
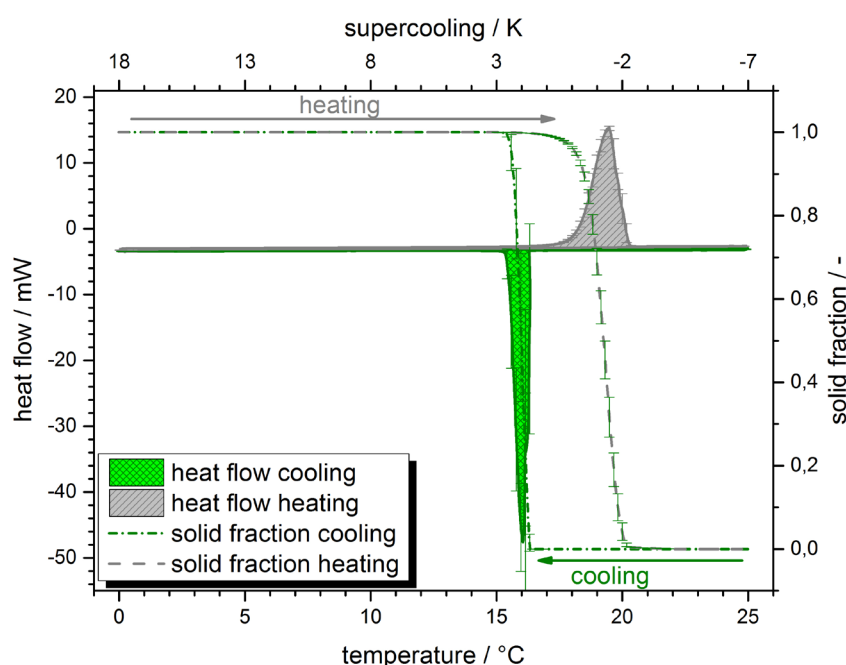
Figure 3. Differential scanning calorimetry (DSC) measurements of bulk hexadecane. Cooling from 25 to 0 °C with cooling rate of 1 K/min: the grid area is the integral of the cooling curve with the dot chain line for solid fraction as a function of temperature during cooling. Heating from 0 to 25 °C with heating rate of 1 K/min: hatched area is the integral of the heating curve with the dash line for solid fraction as a function of temperature during heating.

The determination of solid fraction was possible due to the absence of change in the absolute value of phase transition energy and enthalpy during solidification and melting. This ensured that no previously formed hexadecane crystals (no increase of solid–liquid phase transition energy compared to liquid–solid phase transition energy) or foreign crystals were present in the samples (the determined crystallization and melting enthalpy equals the literature fusion enthalpy value of -227.26 J/g for hexadecane [36]).

Similar to bulk hexadecane, 1 wt % hexadecane oil-in-water emulsions showed sharp exothermic peaks during cooling, and broader endothermic peaks during heating. Since the amount of hexadecane was only 1 wt %, the heat flow signal was particularly low (see Figure 4).

Table 1. Evaluation of phase transition onset temperature, energy and enthalpy of thermal analysis measurements of bulk hexadecane and of 1 wt % hexadecane in Milli-Q water emulsions stabilized with 1 wt % Tween® 20 according to Figures 3 and 4.

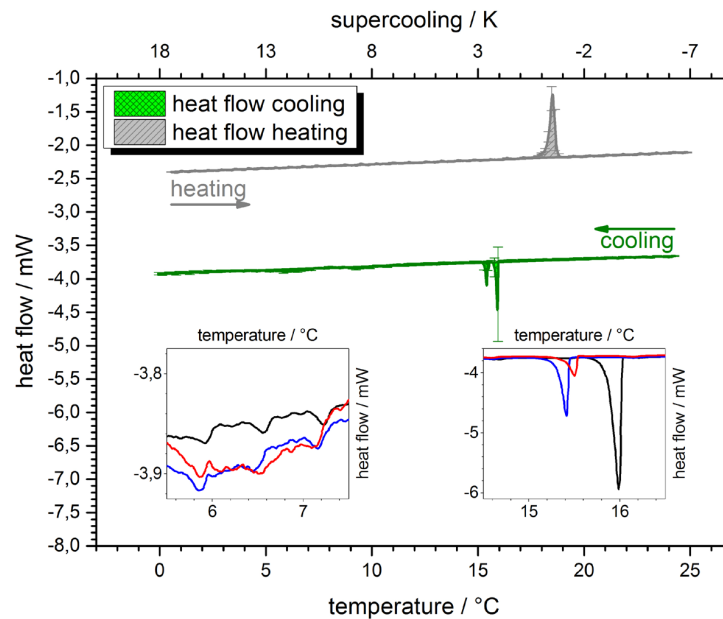| Phase Transition	Temperature/°C	Energy/mJ	Enthalpy/J/g
liquid–solid transition of the bulk	16.21 ± 0.12	-1281.47 ± 5.11	-230.65 ± 0.37
solid–liquid transition of the bulk	18.26 ± 0.05	$+1279.50 \pm 7.44$	$+230.11 \pm 0.34$
liquid–solid transition of the emulsion	15.66 ± 0.32	-6.98 ± 6.16	-0.67 ± 0.61
solid–liquid transition of the emulsion	18.33 ± 0.01	17.60 ± 1.48	1.78 ± 0.18

Figure 4. DSC measurements of 1 wt % hexadecane in Milli-Q water emulsions stabilized with 1 wt % Tween® 20. Cooling from 25 to 0 °C with cooling rate of 1 K/min: grid area is the integral of cooling curve and standard deviation of the repetitions. Heating from 0 to 25 °C with heating rate of 1 K/min: hatched area is the integral of heating curve and standard deviation of the repetitions. The outlined region from 15 to 16 °C on the right shows the major crystallization peaks of the measured emulsion. The outlined region from 6 to 7 °C on the left shows magnified cooling curves of the measured emulsions.

In the case of 1 wt % hexadecane oil-in-water emulsions, the onset crystallization temperature was 15.66 °C ($\pm$0.32 K) and thus lower than the crystallization temperature of bulk hexadecane (see Table 1). This is caused by the reduction of catalytic impurities within decreasing droplet volumes [1,34]. Also during melting, hexadecane oil-in-water emulsions showed a slightly higher melting temperature of 18.33 °C ($\pm$0.01 K) compared to bulk hexadecane.

The determination of solid fraction using DSC measurements of hexadecane oil-in-water emulsions was not possible. The integration of heat flow curves led to different initial values of phase transition energies as shown in Table 1. Since crystallization in droplets is a stochastic process, solidification of single emulsion droplets may occur at different stages of supercooling. Melting of the droplets, on the other hand, occurs near the melting point of bulk hexadecane and may be marginally affected by the droplet size and thermodynamic properties of the system. The higher melting energy compared to the crystallization energy led to the assumption that not every crystallization event that took place could be recorded in a heat flow curve during DSC measurements. The comparison of the solid–liquid phase transition enthalpies of bulk hexadecane (230.11 J/g) and hexadecane oil-in-water emulsions (1.78 J/g) also demonstrated many non-detected melting events: Here, the transition energy

of the 1 wt % hexadecane oil-in-water emulsion should be in the range of about one hundredth of the solid–liquid transition enthalpy of bulk hexadecane (2.30 J/g).

To detect every crystallization and melting event within droplets, we investigated hexadecane oil-in-water emulsions under a cryo polarizing microscope equipped with an optically accessible precise cooling/heating stage. In this manner, we were able to optically follow the crystallization of single droplets in droplet clusters at the same temperature conditions as previously described in the DSC measurements. Due to the polarization filter, it was possible to differentiate between liquid or supercooled droplets (gray, transparent), amorphous particles (gray, turbid) and mono (colored, transparent) or multi crystalline (colored, opaque) structures.

Using our model system, 1 wt % hexadecane in Milli-Q water emulsion stabilized with 1 wt % Tween® 20, we observed three different states of the dispersion during supercooling: liquid droplets above 18 °C (gray, transparent), supercooled droplets below 18 °C (gray, transparent) and multi crystalline (colored, opaque) structures (see Figure 5). No amorphous particles (gray, turbid) or mono crystalline structures (colored, transparent) were observed during the experiments with this model system. The observed dense monolayer arrangement of droplets, despite the low dispersed phase mass fraction, was caused by creaming of droplets in the measurement cell. Hexadecane droplets crystallized as multi crystalline spheroids and remained nearly spherical after solidification. Crystallized droplets were detected first at 15.30 °C (±0.16 K) which is similar to the onset crystallization temperature of 15.66 °C (±0.32 K) measured by DSC. At 15 °C (3 K supercooling) further crystalized droplets were detected, which crystallized individually and stochastically distributed in the observed volume. The individual crystallization behavior of droplets in droplet clusters might be the reason for the difficulties in detecting crystallization events during DSC measurements and, consequently, calculation of solid fraction in emulsions with low dispersed phase mass fraction.
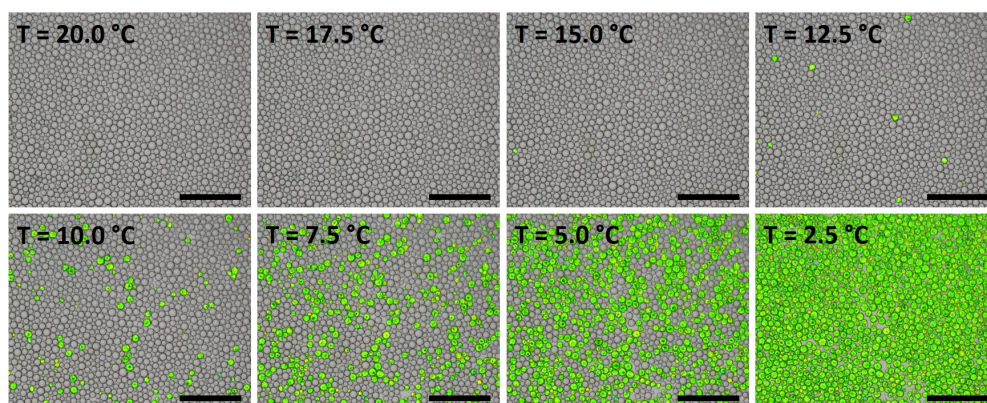

Figure 5. Micrographs of 1 wt % hexadecane in Milli-Q water emulsion stabilized with 1 wt % Tween® 20. Cooling from 28 to 0 °C with cooling rate of 1 K/min: gray transparent spheres are liquid or supercooled droplets and green opaque spheroids are multi crystalline structures of solidified hexadecane droplets. With decreasing temperature, the number of solidified droplets increases. Length of the scale bar is 200 μm.

Decreasing the temperature led to an increasing number of crystallized droplets. Different to crystallization at low supercooling, at higher supercooling droplets tended to crystallize in the neighborhood of already solidified droplets, as can be observed in Figure 5, during the temperature decrease from 10 °C (8 K supercooling) to 5.0 °C (13 K supercooling). We propose that secondary nucleation was initiated in supercooled droplets in contact with crystallized droplets, which can be compared, in attenuated form, to the collision-mediated secondary nucleation in hexadecane oil-in-water emulsions [18]. A complete crystallization of droplets in 1 wt % hexadecane oil-in-water emulsions was observed at 2.20 °C (±0.14 K).

The discrepancy of the calorimetric measurements and thermo-optical investigations of crystallization behavior in emulsions at low dispersed phase fraction is mostly influenced by the following factors: (1) determination by number (thermo-optical investigations) vs. determination by mass (calorimetric measurements); (2) technical limitations (signal to noise ratio); and (3) statistical effects (analyzed sample volume). As it already known, big droplets tend to crystallize at low supercooling near the crystallization temperature of the bulk, while small droplets lead to large supercooling until crystallization [1]. The droplet size in the model hexadecane emulsion system ranges from 2.6 to 44.9 μm (see Figure 6, laser diffraction measurements). The evaluation of crystallization events in these droplets by number leads to signal ratio of 1 (2.6 μm droplet) to 1 (44.9 μm droplet), while the evaluation by mass generates a signal ratio of 1 (2.6 μm droplet) to approx. 5000 (44.9 μm droplet). Therefore, crystallization of single big droplets causes large crystallization peaks near the bulk crystallization temperatures (shown in Figure 4, outlined region between 15 and 16 °C), while individual crystallization of small droplets at high supercoolings generates low signal leading to a bad signal-to-noise ratio (shown in Figure 4, outlined region between 6 and 7 °C). Additionally, statistical effects, caused by different sample volumes (calorimetric measurements: 5 mg vs. thermo-optical investigation: between 0.05 and 0.5 mg in the observed volume), influence the probability of big droplets in the sample: small sample volume implies low probability of big droplets in the sample, causing low signal by mass; high sample volume implies high probability of big droplets in the sample, causing high signal by mass. Consequently, evaluation by number, especially at low dispersed phase fraction, is less sensitive to this phenomenon.
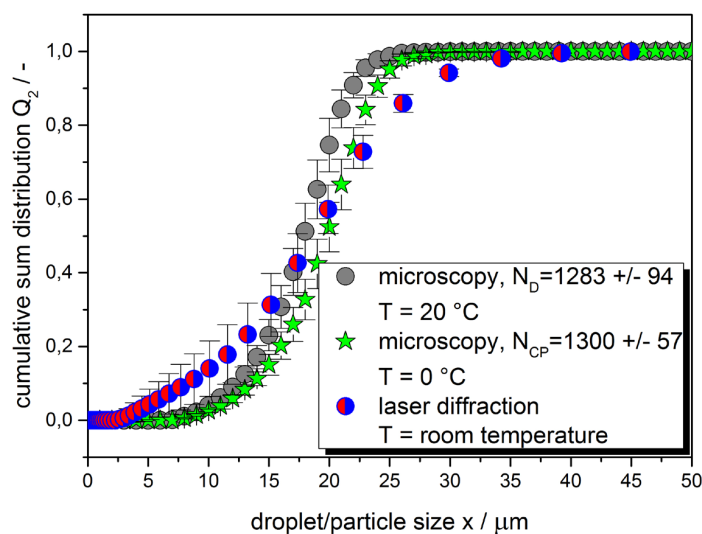

Figure 6. Cumulative area sum distribution Q_2 of 1 wt % hexadecane in Milli-Q water emulsions stabilized with 1 wt % Tween® 20. Filled circles, one color: DSD measurements with polarizing microscope at 20 °C of liquid droplets. Filled stars, one color: Particles size distribution (PSD) measurements with polarizing microscope at 0 °C of crystallized droplets. Filled circles, bicolor: DSD measurements using laser diffraction and Mie theory at room temperature (above melting point of hexadecane) of liquid droplets.

The size distribution of liquid droplets before crystallization at 20 °C and after the entire crystallization of droplets at 0 °C was determined from the micrographs as described in Material and Methods. In addition, laser diffraction measurements of liquid droplets at room temperature (above the melting point of hexadecane) were performed. All distributions are shown in Figure 6. We observed a slight increase of the size distribution during the liquid–solid transition of droplets. However, we can confirm that no coalescence events took place during phase transition in all of our thermo-optical experiments. Consequently, the number of droplets before crystallization (N_d = 1283, ±94) and

the number of resulting crystallized particles after solidification (N_{cp} = 1300, $\pm$57) were identical within standard deviation. A change in the total evaluated number of droplets/particles during phase transition was caused by a slight movement of droplets/particles out of the observation area. Compared to the more statistical laser diffraction and Mie theory based droplet size distribution measurements, we can see that both cumulative sum distribution curves (polarized microscopy and laser diffraction) intersect at the same mean value $x_{50.2}$ ($x_{50.2, \text{microscopy}}$ = 17.64 μm and $x_{50.2, \text{laser diffraction}}$ = 17.46 μm). Thus, the deviation in $x_{10.2}$ and $x_{90.2}$ values are the result of the evaluation of a larger amount of emulsion droplets in case of laser diffraction (several thousand droplets), while only a reduced amount of droplets can be analyzed in case of thermo-optical polarized microscopy due to the limited observation area (range here: one thousand droplets). Nevertheless, comparing mean values $x_{50.2}$ leads to an excellent match in size evaluation of emulsions.

The direct thermo-optical method can also be used to characterize individual crystallization in droplets and droplet clusters and to differentiate between the solid and the crystalline fraction at a specific temperature or during supercooling, respectively. The total number of crystalline particles in relation to the total number of particles and droplets was taken to calculate the number based crystallization index CI_N:

$$CI_N = \frac{\text{number of crystalline particles}}{\text{total number of particles and droplets}} = \frac{N_{cp}}{N_p + N_d} \tag{1}$$

where N_{cp} is the total number of crystalline particles (mono and multi crystalline structures), N_p the total number of solid particles (amorphous, mono and multi crystalline structures) and N_d the total number of droplets (liquid and supercooled droplets). Depending on the application, CI_i may also be given as the relation between mass (CI_M) or volume (CI_V) of the investigated material, both of which can be calculated from the micrographs. As crystallization in emulsions is an event taking place in single droplets, and since we always observed immediate and entire crystallization within a droplet after nucleation, we concentrate on the number based CI_N for the following discussions.

The total number of droplets/particles, droplet/particle size, and size distribution were determined as a function of temperature and supercooling with simultaneous differentiation in physical state of droplets (liquid and supercooled liquid) and particles (amorphous solid, mono crystalline solid, and multi crystalline solid). As shown in Figure 5, hexadecane emulsions formed multi crystalline spheroids during liquid–solid transition, which limited the differentiation to supercooled liquid and multi crystalline spheroids during the determination of crystallization index shown in Figure 7.
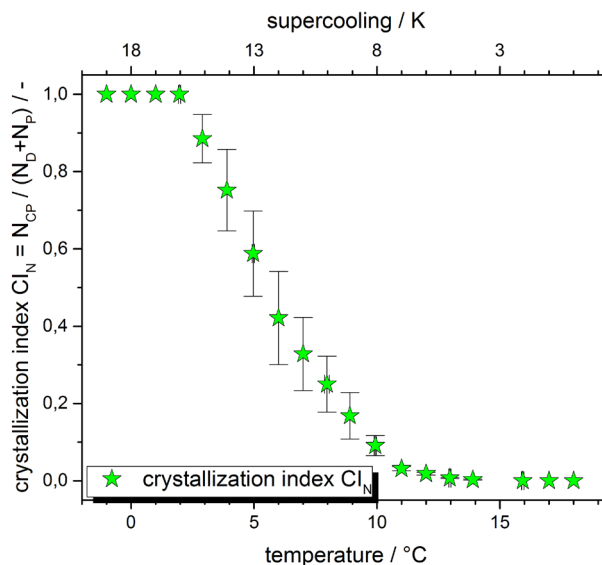
Figure 7. Number based crystallization index CI_N as function of temperature and supercooling of 1 wt % hexadecane in Milli-Q water emulsions stabilized with 1 wt % Tween® 20.

Different to DSC measurements, every crystallization event had been recorded in the observed volume during thermo-optical investigation of hexadecane oil-in-water emulsions. As shown in Figure 4 and Table 1, the highest heat flow signal of DSC was detected at 15.66 °C (±0.32 K). At this temperature (at 15.30 °C, ±0.16 K), first crystallization events within droplets were detected during thermo-optical observation. However, at this temperature, the crystallization process within supercooled droplets was only initialized, as can be seen in Figure 5. In the range from 15 °C (3 K supercooling) to 12.5 °C (5.5 K supercooling), only a few droplets crystallized individually and stochastically within the emulsion. Consequently, CI_N is very low at this temperature range (see Figure 7). Between 12.5 °C and 10 °C (8 K supercooling), we see a transition region with an increasing number of crystallization events within droplets and an exponential increase of crystallized droplets until 2.2 °C (±0.14 K, 15.8 K supercooling). From 2.2 °C on, all droplets in the investigated sample volume were observed in the form of multi crystalline spheroids.

A more detailed analysis of the crystallization index as a function of formulation (materials and concentrations) and process (shear and external forces) parameters is the subject of ongoing work and will be discussed in detail in our following papers.

4. Conclusions

The application properties of oil-in-water emulsions with crystalline dispersed phase depend strongly on the crystallization step within the droplets. Different to crystallization of bulk materials, oil-in-water emulsions show individual crystallization of droplets which differs from droplet to droplet. Consequently, non-integral methods are required to describe the crystallization behavior of single droplets and of droplets in droplet clusters such as oil-in-water emulsions. In this contribution, we presented a direct thermo-optical procedure that we developed to describe the crystallization progress within oil-in-water micro emulsions. The use of a polarizing microscope equipped with a precise cooling/heating stage enabled us to gain insight into the crystallization behavior in concentrated emulsions. At the same time, the detection and characterization of individual crystallization events in single droplets (range 1 μm to several hundred μm) in droplet clusters was possible. Simultaneously, precise differentiation between liquid, supercooled liquid, amorphous, and mono or multi crystalline structures allowed for the introduction of a crystallization index CI_i. Due to the high degree of detail of this method, the number based CI_N specifies the ratio of crystalline structures to total number of structures and can differentiate between different types of solid fractions

(amorphous and mono or multi crystalline structures). Compared to conventional thermal analysis using differential scanning calorimetry, more detailed information about crystallization behavior of emulsions can thus be achieved. We applied this thermo-optical analysis to a hexadecane oil-in-water model emulsion stabilized with Tween® 20. We could thus show that crystallization only took place in the dispersed phase of the hexadecane oil-in-water emulsions without any sign of crystal formation in the continuous phase and crystallization of the continuous phase itself. We saw a slight increase in size distribution during liquid–solid phase transition and could exclude coalescence as the reason for this increase due to the simultaneous number monitoring of emulsion droplets during phase transition. In addition to the determination of the number based CI_N of hexadecane oil-in-water emulsions, our thermo-optical procedure delivered detailed information on number, size, size distribution, and morphology of the dispersed phase and its change during the phase transition in a single measurement using only one analytical device.

Author Contributions: Serghei Abramov and Heike Petra Schuchmann conceived and designed the experiments; Serghei Abramov and Patrick Ruppik performed the experiments; Serghei Abramov and Patrick Ruppik analyzed the data; Serghei Abramov and Heike Petra Schuchmann wrote the paper.

Conflicts of Interest: The authors declare no conflict of interest. The founding sponsors had no role in the design of the study; in the collection, analyses, or interpretation of data; in the writing of the manuscript, and in the decision to publish the results.

Abbreviations

The following abbreviations are used in this manuscript:

CI_i	Crystallization index
CI_N	Number based crystallization index
CI_M	Mass based crystallization index
CI_V	Volume based crystallization index
DSC	Differential scanning calorimetry
DSD	Droplet size distribution
PSD	Particles size distribution

References

1. McClements, D.J. Crystals and crystallization in oil-in-water emulsions: Implications for emulsion-based delivery systems. *Adv. Colloid Interface Sci.* **2012**, *174*, 1–30. [CrossRef] [PubMed]
2. Pardeike, J.; Hommoss, A.; Müller, R.H. Lipid nanoparticles (SLN, NLC) in cosmetic and pharmaceutical dermal products. *Int. J. Pharm.* **2009**, *366*, 170–184. [CrossRef] [PubMed]
3. Müller, R. Solid lipid nanoparticles (SLN) for controlled drug delivery—A review of the state of the art. *Eur. J. Pharm. Biopharm.* **2000**, *50*, 161–177. [CrossRef]
4. Humberstone, A.J.; Charman, W.N. Lipid-based vehicles for the oral delivery of poorly water soluble drugs. *Adv. Drug Deliv. Rev.* **1997**, *25*, 103–128. [CrossRef]
5. McClements, D.J.; Decker, E.A.; Weiss, J. Emulsion-based delivery systems for lipophilic bioactive components. *J. Food Sci.* **2007**, *72*, R109–R124. [PubMed]
6. Rostami, E.; Kashanian, S.; Azandaryani, A.H.; Faramarzi, H.; Dolatabadi, J.E.N.; Omidfar, K. Drug targeting using solid lipid nanoparticles. *Chem. Phys. Lipids* **2014**, *181*, 56–61. [CrossRef] [PubMed]
7. Coupland, J.N. Crystallization in emulsions. *Curr. Opin. Colloid Interface Sci.* **2002**, *7*, 445–450.
8. McClements, D.J.; Li, Y. Structured emulsion-based delivery systems: Controlling the digestion and release of lipophilic food components. *Adv. Colloid Interface Sci.* **2010**, *159*, 213–228. [CrossRef] [PubMed]
9. Köhler, K., Schuchmann, H.P. (Eds.) *Emulgiertechnik: Grundlagen, Verfahren und Anwendungen*; 3. Aufl.; Behr: Hamburg, Germany, 2012.
10. Mehnert, W. Solid lipid nanoparticles Production, characterization and applications. *Adv. Drug Deliv. Rev.* **2001**, *47*, 165–196. [PubMed]
11. Wissing, S.A.; Kayser, O.; Müller, R.H. Solid lipid nanoparticles for parenteral drug delivery. *Adv. Drug Deliv. Rev.* **2004**, *56*, 1257–1272. [CrossRef] [PubMed]

12. Köhler, K.; Hensel, A.; Kraut, M.; Schuchmann, H.P. Melt emulsification—Is there a chance to produce particles without additives? *Particuology* **2011**, *9*, 506–509. [CrossRef]

13. Himawan, C.; Starov, V.M.; Stapley, A.G.F. Thermodynamic and kinetic aspects of fat crystallization. *Adv. Colloid Interface Sci.* **2006**, *122*, 3–33. [CrossRef] [PubMed]

14. Vanapalli, S.A.; Coupland, J.N. Emulsions under shear—The formation and properties of partially coalesced lipid structures. *Food Hydrocoll.* **2001**, *15*, 507–512. [CrossRef]

15. Helgason, T.; Awad, T.S.; Kristbergsson, K.; McClements, D.J.; Weiss, J. Effect of surfactant surface coverage on formation of solid lipid nanoparticles (SLN). *J. Colloid Interface Sci.* **2009**, *334*, 75–81. [CrossRef] [PubMed]

16. Bolzinger, M.A.; Cogne, C.; Lafferrere, L.; Salvatori, F.; Ardaud, P.; Zanetti, M.; Puel, F. Effects of surfactants on crystallization of ethylene glycol distearate in oil-in-water emulsion. *Colloids Surf. A Physicochem. Eng. Asp.* **2007**, *299*, 93–100. [CrossRef]

17. Povey, M.J.W.; Awad, T.S.; Huo, R.; Ding, Y. Quasi-isothermal crystallisation kinetics, non-classical nucleation and surfactant-dependent crystallisation of emulsions. *Eur. J. Lipid Sci. Technol.* **2009**, *111*, 236–242. [CrossRef]

18. Hindle, S.; Povey, M.J.; Smith, K. Kinetics of Crystallization in *n*-Hexadecane and Cocoa Butter Oil-in-Water Emulsions Accounting for Droplet Collision-Mediated Nucleation. *J. Colloid Interface Sci.* **2000**, *232*, 370–380. [CrossRef] [PubMed]

19. Yang, D.; Hrymak, A.N.; Kamal, M.R. Crystal Morphology of Hydrogenated Castor Oil in the Crystallization of Oil-in-Water Emulsions: Part II. Effect of Shear. *Ind. Eng. Chem. Res.* **2011**, *50*, 11594–11600. [CrossRef]

20. Da Pieve, S.; Calligaris, S.; Co, E.; Nicoli, M.C.; Marangoni, A.G. Shear Nanostructuring of Monoglyceride Organogels. *Food Biophys.* **2010**, *5*, 211–217. [CrossRef]

21. Bunjes, H. Structural properties of solid lipid based colloidal drug delivery systems. *Curr. Opin. Colloid Interface Sci.* **2011**, *16*, 405–411. [CrossRef]

22. Weiss, J.; Decker, E.A.; McClements, D.J.; Kristbergsson, K.; Helgason, T.; Awad, T. Solid Lipid Nanoparticles as Delivery Systems for Bioactive Food Components. *Food Biophys.* **2008**, *3*, 146–154. [CrossRef]

23. Schugens, C.; Laruelle, N.; Nihant, N.; Grandfils, C.; Jérome, R.; Teyssié, P. Effect of the emulsion stability on the morphology and porosity of semicrystalline poly l-lactide microparticles prepared by *w/o/w* double emulsion-evaporation. *J. Control. Release* **1994**, *32*, 161–176. [CrossRef]

24. Greaves, D.; Boxall, J.; Mulligan, J.; Sloan, E.D.; Koh, C.A. Hydrate formation from high water content-crude oil emulsions. *Chem. Eng. Sci.* **2008**, *63*, 4570–4579. [CrossRef]

25. Saggin, R.; Coupland, J.N. Measurement of solid fat content by ultrasonic reflectance in model systems and chocolate. *Food Res. Int.* **2002**, *35*, 999–1005. [CrossRef]

26. Saggin, R.; Coupland, J.N. Shear and longitudinal ultrasonic measurements of solid fat dispersions. *J. Am. Oil Chem. Soc.* **2004**, *81*, 27–32. [CrossRef]

27. Yang, D.; Hrymak, A.N. Crystal Morphology of Hydrogenated Castor Oil in the Crystallization of Oil-in-Water Emulsions: Part I. Effect of Temperature. *Ind. Eng. Chem. Res.* **2011**, *50*, 11585–11593. [CrossRef]

28. Khalil, A.; Puel, F.; Cosson, X.; Gorbatchev, O.; Chevalier, Y.; Galvan, J.-M.; Rivoire, A.; Klein, J.-P. Crystallization-in-emulsion process of a melted organic compound: In situ optical monitoring and simultaneous droplet and particle size measurements. *J. Cryst. Growth* **2012**, *342*, 99–109. [CrossRef]

29. Julian McClements, D.; Dickinson, E.; Povey, M.J.W. Crystallization in hydrocarbon-in-water emulsions containing a mixture of solid and liquid droplets. *Chem. Phys. Lett.* **1990**, *172*, 449–452. [CrossRef]

30. Palanuwech, J. A method to determine free fat in emulsions. *Food Hydrocoll.* **2003**, *17*, 55–62. [CrossRef]

31. Karanjkar, P.U.; Lee, J.W.; Morris, J.F. Calorimetric investigation of cyclopentane hydrate formation in an emulsion. *Chem. Eng. Sci.* **2012**, *68*, 481–491. [CrossRef]

32. McClements, D.J.; Dungan, S.R.; German, J.B.; Simoneau, C.; Kinsella, J.E. Droplet Size and Emulsifier Type Affect Crystallization and Melting of Hydrocarbon-in-Water Emulsions. *J. Food Sci.* **1993**, *58*, 1148–1151. [CrossRef]

33. Awad, T.S.; Moharram, H.A.; Shaltout, O.E.; Asker, D.; Youssef, M.M. Applications of ultrasound in analysis, processing and quality control of food: A review. *Food Res. Int.* **2012**, *48*, 410–427. [CrossRef]

34. Herhold, A.B.; Ertaş, D.; Levine, A.J.; King, H.E. Impurity mediated nucleation in hexadecane-in-water emulsions. *Phys. Rev. E* **1999**, *59*, 6946–6955. [CrossRef]

35. Stieß, M. *Mechanische Verfahrenstechnik—Partikeltechnologie 1*; Stieß, M., Ed.; 3., vollst. neu bearb. Aufl.; Springer: Berlin/Heidelberg, Germany, 2009.

36. Domalski, E.S.; Hearing, E.D. Heat Capacities and Entropies of Organic Compounds in the Condensed Phase. Volume III. *J. Phys. Chem. Ref. Data* **1996**, *25*. [CrossRef]